Journal of Physics: Conference Series **446** (2013) 012056 doi:10.1088/1742-6596/446/1/012056

# Hadronic resonances at ALICE

**A G Knospe (for the ALICE Collaboration)**

Department of Physics, The University of Texas at Austin, 1 University Station C1600, Austin, TX 78712-0264 USA

E-mail: anders.knospe@cern.ch

**Abstract.** Measurements of the ratios of hadronic resonance yields to non-resonance yields can be used to study the properties of the hadronic phase of high-energy heavy-ion collisions. A change in resonance masses or widths could be an indication of chiral symmetry restoration. Measurements of resonances in proton-proton collisions provide an important baseline for measurements in heavy-ion collisions as well as data for tuning QCD-inspired particle production models. The ALICE collaboration has measured the $\mathrm{K}^*(892)^0$ and $\phi(1020)$ resonances in Pb–Pb collisions at $\sqrt{s_{\mathrm{NN}}} = 2.76$ TeV and the $\mathrm{K}^*(892)^0$, $\phi(1020)$, and $\Sigma^*(1385)^{\pm}$ resonances in pp collisions at $\sqrt{s} = 7$ TeV. These measurements – including transverse momentum spectra, ratios to non-resonances, masses, and widths – are discussed and compared to theoretical predictions.

## 1. Introduction

These proceedings report measurements of resonances in pp collisions at $\sqrt{s} = 7$ TeV and Pb–Pb collisions at $\sqrt{s_{\mathrm{NN}}} = 2.76$ TeV. The study of resonance production yields in pp collisions provides an important baseline for comparison with results in Pb–Pb collisions. Resonance spectra in pp collisions can also be used to tune the predictions of QCD-inspired event generators such as PYTHIA [1] and PHOJET [2].

In nucleus-nucleus collisions, resonances can be used to study the properties of the hadronic phase and to search for the signatures of chiral symmetry restoration in the medium. Resonances may be produced through regeneration in the hadronic phase and the observable resonance signal may be reduced through the re-scattering of the decay daughters [3–6]. Statistical models [4, 7, 8] can be used to predict the ratios of resonance yields to the yields of non-resonances as functions of the chemical freeze-out temperature $T_{\mathrm{ch}}$ and the time $\Delta t$ between chemical and thermal freeze-out; simultaneous measurements of at least two resonance-to-non-resonance ratios (*e.g.*, $\mathrm{K}^{*0}/\mathrm{K}$ and $\Lambda^*(1520)/\Lambda$) may allow constraints to be placed on $T_{\mathrm{ch}}$ and $\Delta t$. It is expected that chiral symmetry will be restored at approximately the same critical temperature as the phase transition to the QGP [9]. Resonances that interact with and decay inside the medium (when chiral symmetry is at least partially restored) may be shifted off-shell and may also have shorter lifetimes than observed in vacuum [10–12]. It is expected [13, 14] that it would be easiest to observe the signatures of chiral symmetry restoration in the range $2 < p_{\mathrm{T}} < 10$ GeV/$c$ at LHC energies, due to regeneration and re-scattering at low $p_{\mathrm{T}}$ and the time dilation of decays for high $p_{\mathrm{T}}$.

The ALICE detector is described in [15]. The analyses described in these proceedings use the Inner Tracking System (ITS, for tracking and vertex finding), the Time Projection Chamber (TPC, for tracking and particle identification through energy loss), the Time-of-Flight

(TOF) detector (for particle identification), and the V0 detector (which provides minimum-bias triggers).

## 2. Resonances in pp Collisions at $\sqrt{s} = 7$ TeV

The analyses of the $\mathrm{K}^{*0}$ and $\phi$ mesons[1] in pp collisions at $\sqrt{s} = 7$ TeV are described in detail in [16]. The $\mathrm{K}^{*0}$ ($\phi$) meson is reconstructed in 80 (60) M minimum-bias pp collisions via the decay channel $\mathrm{K}^{*0} \rightarrow \pi^{\pm}\mathrm{K}^{\mp}$ ($\phi \rightarrow \mathrm{K}^{-}\mathrm{K}^{+}$) which has a branching ratio of 0.666 (0.489) [17]. The decay products of the $\mathrm{K}^{*0}$ are identified using the TOF; the TPC is used if no TOF signal is present. The decay products of the $\phi$ are identified using the TPC, with the addition of TOF information if a signal is present. The invariant-mass distributions of unlike-charge $\pi$K and KK pairs (with $|y_{\mathrm{pair}}| < 0.5$) in the same event are constructed. Two methods are used to estimate the combinatorial background. First, the background is extracted from the distributions of like-charge pairs in the same event. Second, each decay product is paired with unlike-charge tracks from a different event (with a similar primary vertex $z$ position and charged track multiplicity). The like-charge (event mixing) method is the default used for the $\mathrm{K}^{*0}$ ($\phi$) analysis. The background-subtracted $\mathrm{K}^{*0}$ ($\phi$) invariant-mass distributions are fitted with a Breit-Wigner (Voigtian[2]) peak added to a $2^{\mathrm{nd}}$-order polynomial (which describes the residual background). The product of the efficiency and acceptance is extracted from 60 M Monte-Carlo collisions. The systematic uncertainties in the corrected spectra account for variations due to changing the track selection cuts, the combinatorial background, the mass range of the fit, and the order of the residual-background polynomial. The corrected transverse-momentum spectra cover the ranges $0 < p_{\mathrm{T}} < 6$ GeV/$c$ for the $\mathrm{K}^{*0}$ and $0.4 < p_{\mathrm{T}} < 6$ GeV/$c$ for the $\phi$. These spectra are fitted with Lévy-Tsallis functions [18], which are used to extract the mean transverse momentum $\langle p_{\mathrm{T}} \rangle$ and to estimate the $\phi$ meson yield for low $p_{\mathrm{T}}$. The ratios of the $p_{\mathrm{T}}$-integrated $\mathrm{K}^{*0}$ and $\phi$ yields to the yields of charged kaons are calculated.

The $\Sigma^{*\pm}$ and $\overline{\Sigma}^{*\pm}$ baryons are reconstructed in 211 M minimum-bias pp collisions in the rapidity range $|y| < 0.8$ via the decay channel $\Sigma^{*\pm} \rightarrow \pi^{\pm}\Lambda \rightarrow \pi^{\pm}\pi^{-}\mathrm{p}$. The two steps of the decay process have a combined branching ratio of 0.56 [17]. The $\Lambda$ baryons are identified by cuts on their decay topology and invariant mass, and additional topological cuts are applied the $\pi\Lambda$ pairs. The combinatorial background is constructed using the event mixing technique (each $\Lambda$ is paired with a $\pi$ from 5 other events). The residual background is parametrized by the sum of a $3^{\mathrm{rd}}$-order polynomial and a Gaussian, which accounts for correlated $\pi\Lambda$ pairs from $\Lambda^{*}(1520)$ decays. The product of the efficiency and acceptance is calculated using simulated pp collisions. The systematic uncertainties from sources including the track selection cuts, topological cuts, combinatorial background normalization, residual background parametrization, and the material budget in the simulations have been evaluated.

The corrected $\mathrm{K}^{*0}$, $\phi$, and $\frac{1}{2}(\Sigma^{*+} + \overline{\Sigma}^{*-})$ spectra are shown in Figure 1 and compared to predictions from PYTHIA and PHOJET. The PYTHIA Perugia 2011 tune describes the $\mathrm{K}^{*0}$ spectrum and the $\phi$ spectrum for $p_{\mathrm{T}} > 3$ GeV/$c$ well, while the Perugia 0 tune underestimates the spectra. PHOJET and the PYTHIA ATLAS-CSC tune describe the meson spectra for $p_{\mathrm{T}} > 1$ GeV/$c$. The PYTHIA D6T tune deviates from the measured spectra for $p_{\mathrm{T}} > 2$ GeV/$c$. The $\Sigma^{*\pm} + \overline{\Sigma}^{*\mp}$ spectra are well described by the PYTHIA ATLAS-CSC tune for $p_{\mathrm{T}} > 2$ GeV/$c$, while other models under-predict the data.

## 3. Resonances in Pb–Pb Collisions at $\sqrt{s_{\mathrm{NN}}} = 2.76$ TeV

The $\mathrm{K}^{*0}$ ($\phi$) meson is reconstructed in 8.2 (9.5) M Pb–Pb collisions. The decay products are identified using TPC energy loss measurements. For the $\mathrm{K}^{*0}$ ($\phi$) meson, the combinatorial

[1] $\mathrm{K}^{*0}$ refers to both the $\mathrm{K}^{*}(892)^{0}$ and its antiparticle; masses are omitted from all particle symbols

[2] A Breit-Wigner function convoluted with a Gaussian, which accounts for the detector resolution

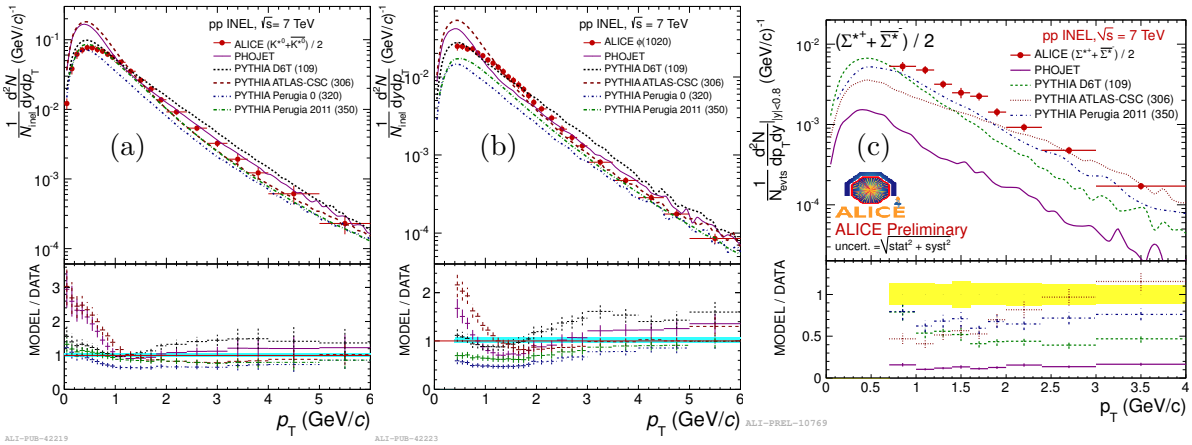


**Figure 1.** Resonance spectra in pp collisions at $\sqrt{s} = 7$ TeV compared to predictions from event generators: $K^{*0}$ (a), $\phi$ (b), $\frac{1}{2}(\Sigma^{*+} + \overline{\Sigma}^{*-})$ (c).

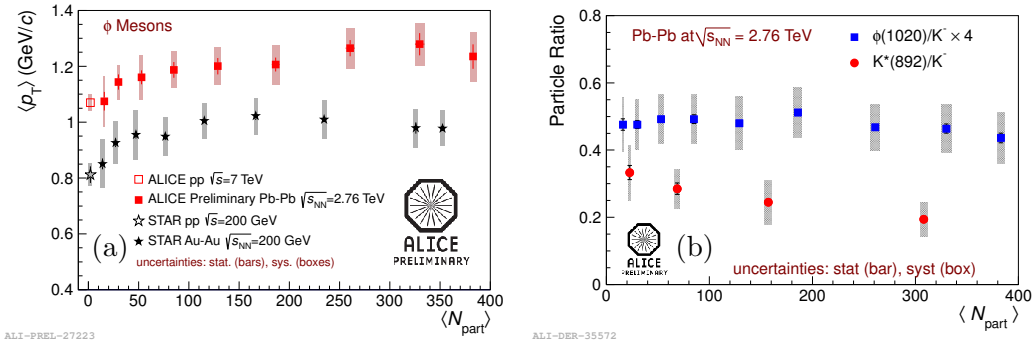


**Figure 2.** (a): Mean transverse momentum for $\phi$ mesons in pp and A–A collisions measured using the ALICE detector and the STAR detector [19, 20]. (b): The $K^{*0}/K^-$ and $\phi/K^-$ ratios measured in Pb–Pb collisions at $\sqrt{s_{\rm NN}} = 2.76$ TeV as functions of $\langle N_{\rm part}\rangle$.

background is calculated using the like-charge (event mixing) method, the residual background is parametrized using a 1st- (2nd-)order polynomial, and the peaks are fit using a Breit-Wigner function. The systematic uncertainties in the corrected spectra account for variations due to changing the track selection cuts, particle identification cuts, the combinatorial background, the mass range of the fit, the order of the residual-background polynomial, and the method used to extract the particle yield (integrating the histogram and subtracting the residual background fit or integrating the peak fit itself). The corrected spectra are fitted with Boltzmann-Gibbs Blast-Wave functions [21]; the $\phi$ meson fits are used to estimate the yields for $p_{\rm T} < 0.5$ GeV/$c$. The values of $\langle p_{\rm T}\rangle$ and the ratios of the $p_{\rm T}$-integrated $K^{*0}$ and $\phi$ yields to the yields of charged kaons [22] are calculated.

The masses and widths of the $K^{*0}$ and $\phi$ mesons were extracted from the Breit-Wigner peak fits. The $K^{*0}$ mass deviates from the vacuum value by about 10 MeV/$c^2$ for $p_{\rm T} < 2$ GeV/$c$. Similar deviations in the $K^{*0}$ mass are observed in pp collisions at $\sqrt{s} = 7$ TeV, suggesting that the deviations in Pb–Pb collisions are instrumental effects ($K^{*0}$ peaks from GEANT simulations are being studied to verify this). Furthermore, the deviation occurs in a momentum range where the fraction of regenerated resonances (which would have vacuum properties) would be large and the signal would be heavily modified by re-scattering [13, 14]. The $K^{*0}$ width is consistent with the vacuum value. The $\phi$ mass (width) deviates from the vacuum value by 0.5 (1-2) MeV/$c^2$. When $\phi$ peaks from GEANT simulations are fitted using the same procedure, similar deviations

from the vacuum value are observed.

The values of $\langle p_{\rm T} \rangle$ for $\phi$ mesons in pp and nucleus-nucleus collisions at RHIC and LHC energies are shown as functions of $\langle N_{\rm part} \rangle$ in Figure 2a. The $\langle p_{\rm T} \rangle$ values measured in pp collisions ($\langle N_{\rm part} \rangle = 2$) at $\sqrt{s} = 7$ TeV are consistent with the values measured in peripheral Pb–Pb collisions at $\sqrt{s_{\rm NN}} = 2.76$ TeV. Higher $\langle p_{\rm T} \rangle$ values are observed for $\rm K^{*0}$ and $\phi$ in A–A collisions at LHC energies than at RHIC [19, 20] energies; increases in $\langle p_{\rm T} \rangle$ from RHIC to LHC energies are also observed [22] for charged pions and kaons and appear to be due to increased radial flow in A–A collisions at LHC energies.

The ratios of the $p_{\rm T}$-integrated yields $\rm K^{*0}/K^-$ and $\phi/\rm K^-$ in Pb–Pb collisions at $\sqrt{s_{\rm NN}} = 2.76$ TeV are shown as functions of $\langle N_{\rm part} \rangle$ in Figure 2b. While the $\phi$/K ratio is independent of centrality, the $\rm K^{*0}$/K ratio decreases for more central collisions (which is an indication that re-scattering effects become larger in central Pb–Pb collisions). The statistical thermal model of Ref. [7] has been used to predict particle yields in central Pb–Pb collisions at $\sqrt{s_{\rm NN}} = 2.76$ TeV, assuming a temperature of 164 MeV. The model prediction (without re-scattering) of $\phi/\rm K^- = 0.128$ is consistent with the measured value, while the prediction of $\rm K^{*0}/K^- = 0.31$ is larger than the measured value. From RHIC [19] to LHC energies, the $\rm K^{*0}$/K and $\phi$/K ratios are independent of $\sqrt{s_{\rm NN}}$; the $\phi$/K ratio is independent of the collision system.

## 4. Conclusions

The spectra of the $\rm K^{*0}$, $\phi$, $\Sigma^{*\pm}$, and $\overline{\Sigma}^{*\pm}$ resonances in pp collisions at $\sqrt{s} = 7$ TeV have been compared to predictions by event generators. The PYTHIA Perugia 2011 tune describes the $\rm K^{*0}$ spectrum and portions of the $\phi$ spectrum well; the PHOJET model and the PYTHIA D6T and ATLAS-CSC tunes describe only portions of the $\rm K^{*0}$ and $\phi$ spectra. The PYTHIA ATLAS-CSC tune describes the $\frac{1}{2}(\Sigma^{*\pm} + \overline{\Sigma}^{*\mp})$ spectra for $p_{\rm T} > 2$ GeV/$c$. The values of $\langle p_{\rm T} \rangle$ in Pb–Pb collisions at $\sqrt{s_{\rm NN}} = 2.76$ TeV are observed to be higher than measured at RHIC, consistent with previous observations of larger radial flow at LHC energies. The $\rm K^{*0}/K^-$ ratio decreases for more central Pb–Pb collisions, suggesting that re-scattering effects are larger in central collisions.

## References

[1] Sjöstrand T, Mrenna S and Skands P 2006 *J. High Energy Phys.* **5** 026 1–581
[2] Engel R and Ranft J 1996 *Phys. Rev.* D **54** 4244–62
[3] Bleicher M and Stöcker H 2004 *J. Phys.* G **30** S111–8
[4] Markert C, Torrieri G and Rafelski J 2002 *Proc. of PASI 2002* (*Preprint* `hep-ph/0206260`)
[5] Vogel S and Bleicher M 2005 *Proc. of Nucl. Phys. Winter Meeting 2005 in Bormio* (*Preprint* `nucl-th/0505027v1`)
[6] Bleicher M and Aichelin J 2002 *Phys. Lett.* B **530** 81–7
[7] Andronic A, Braun-Munzinger P and Stachel J 2011 *J. Phys.* G **38** 124081
[8] Torrieri G and Rafelski J 2001 *Phys. Lett.* B **509** 239–45
[9] Petreczky P 2007 *Nucl. Phys.* A **785** 10–7
[10] Rapp R, Wambach J and van Hees H 2009 *Preprint* `0901.3289v1`
[11] Brown G E and Rho M 2002 *Rhys. Rep.* **363** 85–171
[12] Brodsky S J and de Teramond G F 1988 *Phys. Rev. Lett.* **60** 1924–7
[13] Bleicher M *et al* 1999 *J. Phys.* G **25** 1859–96
[14] Markert C, Bellwied R and Vitev I 2008 *Phys. Lett.* B **669** 92–7
[15] Aamodt K *et al* (ALICE Collaboration) 2008 *J. Inst.* **3** No. S08002 i–245
[16] Abelev B *et al* (ALICE Collaboration) 2012 *CERN-PH-EP-2012-221* (*Preprint* `1208.5717v2`)
[17] Beringer J *et al* (Particle Data Group) 2012 *Phys. Rev.* D **86** 010001
[18] Tsallis C 1988 *J. Stat. Phys.* **52** 479
[19] Abelev B I *et al* (STAR Collaboration) 2009 *Phys. Rev.* C **79** 064903
[20] Adams J *et al* (STAR Collaboration) 2005 *Phys. Lett.* B **612** 181–9
[21] Schnedermann E, Sollfrank J and Heinz U 1993 *Phys. Rev.* C **48** 2462–75
[22] Abelev B *et al* (ALICE Collaboration) 2012 *CERN-PH-EP-2012-230* (*Preprint* `1208.1974v1`)